Available online at www.sciencedirect.com
SCIENCE DIRECT®
ELSEVIER
International Journal of Solids and Structures 43 (2006) 1693–1709
INTERNATIONAL JOURNAL OF SOLIDS and STRUCTURES
www.elsevier.com/locate/ijsolstr

Second-order inelastic dynamic analysis of 3-D steel frames

Seung-Eock Kim *, Cuong Ngo-Huu, Dong-Ho Lee

Department of Civil and Environmental Engineering/Construction Tech. Research Institute, Sejong University, 98 Kunja-dong, Kwangjin-ku, Seoul, 143-747, South Korea

Received 30 November 2004; received in revised form 19 May 2005
Available online 20 July 2005

Abstract

This paper presents a reliable numerical procedure for nonlinear time-history analysis of three-dimensional steel frames subjected to dynamic loads. Geometric nonlinearities of member (P-δ) and frame (P-Δ) are taken into account by the use of stability functions in framed stiffness matrix formulation. The gradual yielding along the member length and over the cross-section is included by using a tangent modulus concept and a softening plastic hinge model based on a modified version of Orbison yield surface. A computer program utilizing the average acceleration method for the integration scheme is developed to numerically solve the equation of motion of framed structure formulated in an incremental form. The results of several numerical examples are compared with those derived from using beam element model of ABAQUS program to illustrate the accuracy and the computational efficiency of the proposed procedure.

Keywords: Dynamic analysis; Geometric and material nonlinearities; Plastic hinges; Stability functions; Three-dimensional steel frames

1. Introduction

The second-order inelastic static analysis of three-dimensional steel frames has been studied extensively in recent years together with the rapid development of computer technology. The finite element method using the interpolation functions and the fiber approach for representing the second-order effect and the spread of plasticity is performed by Izzuddin and Smith (1996), Teh and Clark (1999), and Jiang et al. (2002). Although it can include the interaction between normal and shear stresses and its solution is considered to be accurate, it has not been applied widely for daily use in office engineering design because of its

* Corresponding author. Tel.: +82 2 3408 3291; fax: +82 2 3408 3332.
E-mail address: sekim@sejong.ac.kr (S.-E. Kim).

0020-7683/$ - see front matter © 2005 Elsevier Ltd. All rights reserved.
doi:10.1016/j.ijsolstr.2005.06.018

highly computational cost. A more simple and efficient method is the beam-column method using stability functions and refined plastic-hinge approach proposed by Liew et al. (2000) and Kim et al. (2002, 2003, 2001). The benefits of using this method are that they enable only one or two elements to relatively accurately predict the nonlinear response of each framed member and, hence, to save computational time.

The studies on the second-order inelastic dynamic time-history analysis of three-dimensional steel frames are relatively few compared with those of static analysis. Porter and Powell (1971) used a single yield surface to model the abrupt yielding from completely elastic to completely perfectly plastic state of the member ends, and geometric nonlinearity was ignored in the dynamic analysis of three-dimensional pipe frames. Campbell (1994) developed a three-dimensional fiber plastic hinge beam-column element for the second-order inelastic dynamic analysis of framed structures. The geometric nonlinearity caused by axial force was included, but that caused by the interaction between axial force and bending moments was neglected. This method overestimates the strength and stiffness of the member subjected to significant axial force. Chan (1996) used an updated Lagrangian formulation for the large deflection dynamic analysis of space frames, but did not consider the yielding of the material. Al-Bermani and Zhu (1996) also used an updated Lagrangian formulation and a bounding-surface kinematic hardening material model in conjunction with the lumped plasticity assumption. However, this elastoplastic method overpredicts the capacity of stocky members since it neglects to consider the gradual reduction of stiffness as yielding progresses through and along the member. Chi et al. (1998) and El-Tawil and Deierlein (2001) presented a computer program for dynamic analysis of mixed frame structures comprised of steel, reinforced concrete, and/or composite members. Three-dimensional beam-columns were modeled using a flexibility-based distributed plasticity formulation that utilized a bounding surface to model inelastic member cross-section response. The geometric nonlinear behavior was modeled through an updated Lagrangian geometric stiffness approach. Recently, the OpenSees finite element open source software has developed by McKenna et al. (2005) to simulate the response of structural and geotechnical systems subjected to earthquake loading. The three-dimensional nonlinear beam-column elements formulated by force- and displacement-based approaches include both concentrated and distributed plasticity types using the numerical integration method. Geometric nonlinearity effect is included by the use of the corotational coordinate transformation technique. For the last two studies mentioned, the members of structure need to be divided into many elements to capture the second-order effect accurately, and the numerical integration procedure is relatively time-consuming, so the analysis time is relatively long. Therefore, it is not convenient to apply them in a daily practical design.

The purpose of this paper is to extend the application of the stability functions and the refined plastic-hinge approach for second-order inelastic dynamic time-history analysis of three-dimensional frames. Lateral-torsional buckling is assumed to be prevented by adequate lateral bracing. The section of members is assumed to be compact so that it should be able to develop full plastic moment capacity without local buckling; warping torsion is ignored. The material model used is elastic–perfectly plastic. The reduction of torsional stiffness is not considered in plastic hinge. The strain reversal effect is treated by the application of double modulus theory. A computer program utilizing the average acceleration method for the integration scheme is developed to numerically solve the equation of motion of framed structure formulated in an incremental form. Several examples are presented to prove the robustness of the proposed numerical procedure in predicting the dynamic response of three-dimensional framed structures.

2. Formulation

2.1. Stability functions accounting for second-order effects

Stability functions are used to capture the second-order effects since they can account for the effect of the axial force on the bending stiffness reduction of a member. As presented by Kim et al. (2001), the

force–displacement equation using stability functions may be written for three-dimensional beam-column element as

$$\begin{Bmatrix} P \\ M_{y\mathrm{A}} \\ M_{y\mathrm{B}} \\ M_{z\mathrm{A}} \\ M_{z\mathrm{B}} \\ T \end{Bmatrix} = \begin{bmatrix} \frac{EA}{L} & 0 & 0 & 0 & 0 & 0 \\ 0 & S_1\frac{EI_y}{L} & S_2\frac{EI_y}{L} & 0 & 0 & 0 \\ 0 & S_2\frac{EI_y}{L} & S_1\frac{EI_y}{L} & 0 & 0 & 0 \\ 0 & 0 & 0 & S_3\frac{EI_z}{L} & S_4\frac{EI_z}{L} & 0 \\ 0 & 0 & 0 & S_4\frac{EI_z}{L} & S_3\frac{EI_z}{L} & 0 \\ 0 & 0 & 0 & 0 & 0 & \frac{GJ}{L} \end{bmatrix} \begin{Bmatrix} \delta \\ \theta_{y\mathrm{A}} \\ \theta_{y\mathrm{B}} \\ \theta_{z\mathrm{A}} \\ \theta_{z\mathrm{B}} \\ \phi \end{Bmatrix} \tag{1}$$

where P, $M_{y\mathrm{A}}$, $M_{y\mathrm{B}}$, $M_{z\mathrm{A}}$, $M_{z\mathrm{B}}$, and T are axial force, end moments with respect to y and z axes, and torsion, respectively; δ, $\theta_{y\mathrm{A}}$, $\theta_{y\mathrm{B}}$, $\theta_{z\mathrm{A}}$, $\theta_{z\mathrm{B}}$, and ϕ are the axial displacement, the joint rotations, and the angle of twist; A, I_y, I_z, and L are area, moment of inertia with respect to y and z axes, and length of beam-column element; E, G, and J are elastic modulus, shear modulus, and torsional constant of material; S_1, S_2, S_3, and S_4 are the stability functions with respect to y and z axes, respectively, and are presented as

$$S_1 = \begin{cases} \dfrac{\pi\sqrt{\rho_y}\sin\left(\pi\sqrt{\rho_y}\right) - \pi^2\rho\cos\left(\pi\sqrt{\rho_y}\right)}{2 - 2\cos\left(\pi\sqrt{\rho_y}\right) - \pi\sqrt{\rho_y}\sin\left(\pi\sqrt{\rho_y}\right)} & \text{if } P < 0 \\ \dfrac{\pi^2\rho_y\cosh\left(\pi\sqrt{\rho_y}\right) - \pi\sqrt{\rho_y}\sinh\left(\pi\sqrt{\rho_y}\right)}{2 - 2\cosh\left(\pi\sqrt{\rho_y}\right) + \pi\sqrt{\rho_y}\sinh\left(\pi\sqrt{\rho_y}\right)} & \text{if } P > 0 \end{cases} \tag{2a}$$

$$S_2 = \begin{cases} \dfrac{\pi^2\rho_y - \pi\sqrt{\rho_y}\sin\left(\pi\sqrt{\rho_y}\right)}{2 - 2\cos\left(\pi\sqrt{\rho_y}\right) - \pi\sqrt{\rho_y}\sin\left(\pi\sqrt{\rho_y}\right)} & \text{if } P < 0 \\ \dfrac{\pi\sqrt{\rho_y}\sinh\left(\pi\sqrt{\rho_y}\right) - \pi^2\rho_y}{2 - 2\cosh\left(\pi\sqrt{\rho_y}\right) + \pi\sqrt{\rho_y}\sin\left(\pi\sqrt{\rho_y}\right)} & \text{if } P > 0 \end{cases} \tag{2b}$$

$$S_3 = \begin{cases} \dfrac{\pi\sqrt{\rho_z}\sin\left(\pi\sqrt{\rho_z}\right) - \pi^2\rho\cos\left(\pi\sqrt{\rho_z}\right)}{2 - 2\cos\left(\pi\sqrt{\rho_z}\right) - \pi\sqrt{\rho_z}\sin\left(\pi\sqrt{\rho_z}\right)} & \text{if } P < 0 \\ \dfrac{\pi^2\rho\cosh\left(\pi\sqrt{\rho_z}\right) - \pi\sqrt{\rho_z}\sinh\left(\pi\sqrt{\rho_z}\right)}{2 - 2\cosh\left(\pi\sqrt{\rho_z}\right) + \pi\sqrt{\rho_z}\sinh\left(\pi\sqrt{\rho_z}\right)} & \text{if } P > 0 \end{cases} \tag{2c}$$

$$S_4 = \begin{cases} \dfrac{\pi^2\rho_z - \pi\sqrt{\rho_z}\sin\left(\pi\sqrt{\rho_z}\right)}{2 - 2\cos\left(\pi\sqrt{\rho_z}\right) - \pi\sqrt{\rho_z}\sin\left(\pi\sqrt{\rho_z}\right)} & \text{if } P < 0 \\ \dfrac{\pi\sqrt{\rho_z}\sinh\left(\pi\sqrt{\rho_z}\right) - \pi^2\rho_z}{2 - 2\cosh\left(\pi\sqrt{\rho_z}\right) + \pi\sqrt{\rho_z}\sin\left(\pi\sqrt{\rho_z}\right)} & \text{if } P > 0 \end{cases} \tag{2d}$$

where $\rho_y = P/(\pi^2 EI_y/L^2)$, $\rho_z = P/(\pi^2 EI_z/L^2)$, and P is positive for tension.

2.2. CRC tangent modulus model associated with residual stresses

The CRC tangent modulus concept is used to account for gradual yielding (due to residual stresses) along the length of axially loaded members between plastic hinges. The elastic modulus E (instead of moment of inertia I) is reduced to account for the reduction of the elastic portion of the cross-section since the

reduction of the elastic modulus is easier to implement than a new moment of inertia for every different section. From Chen and Lui (1987), the CRC tangent modulus E_t is written as

$$E_t = 1.0E \quad \text{for } P \leqslant 0.5P_y \tag{3a}$$

$$E_t = 4\frac{P}{P_y}E\left(1-\frac{P}{P_y}\right) \quad \text{for } P > 0.5P_y \tag{3b}$$

2.3. Parabolic function for gradual yielding due to flexure

The tangent modulus model is suitable for the member subjected to axial force, but not adequate for cases of both axial force and bending moment. A gradual stiffness degradation model for a plastic hinge is required to represent the partial plastification effects associated with bending. The parabolic function is used to represent the transition from elastic to zero stiffness associated with a developing hinge. From Kim et al. (2001), when the parabolic function for a gradual yielding is active at both ends of an element, the slope–deflection equation may be expressed as

$$\begin{Bmatrix} P \\ M_{y\mathrm{A}} \\ M_{y\mathrm{B}} \\ M_{z\mathrm{A}} \\ M_{z\mathrm{B}} \\ T \end{Bmatrix} = \begin{bmatrix} \frac{E_t A}{L} & 0 & 0 & 0 & 0 & 0 \\ 0 & k_{iiy} & k_{ijy} & 0 & 0 & 0 \\ 0 & k_{ijy} & k_{jjy} & 0 & 0 & 0 \\ 0 & 0 & 0 & k_{iiz} & k_{ijz} & 0 \\ 0 & 0 & 0 & k_{ijz} & k_{jjz} & 0 \\ 0 & 0 & 0 & 0 & 0 & \frac{GJ}{L} \end{bmatrix} \begin{Bmatrix} \delta \\ \theta_{y\mathrm{A}} \\ \theta_{y\mathrm{B}} \\ \theta_{z\mathrm{A}} \\ \theta_{z\mathrm{B}} \\ \phi \end{Bmatrix} \tag{4}$$

where

$$k_{iiy} = \eta_{\mathrm{A}}\left(S_1 - \frac{S_2^2}{S_1}(1-\eta_{\mathrm{B}})\right)\frac{E_t I_y}{L} \tag{5a}$$

$$k_{ijy} = \eta_{\mathrm{A}}\eta_{\mathrm{B}}S_2\frac{E_t I_y}{L} \tag{5b}$$

$$k_{jjy} = \eta_{\mathrm{B}}\left(S_1 - \frac{S_2^2}{S_1}(1-\eta_{\mathrm{A}})\right)\frac{E_t I_y}{L} \tag{5c}$$

$$k_{iiz} = \eta_{\mathrm{A}}\left(S_3 - \frac{S_4^2}{S_3}(1-\eta_{\mathrm{B}})\right)\frac{E_t I_z}{L} \tag{5d}$$

$$k_{ijz} = \eta_{\mathrm{A}}\eta_{\mathrm{B}}S_4\frac{E_t I_z}{L} \tag{5e}$$

$$k_{jjz} = \eta_{\mathrm{B}}\left(S_3 - \frac{S_4^2}{S_3}(1-\eta_{\mathrm{A}})\right)\frac{E_t I_z}{L} \tag{5f}$$

The terms η_{A} and η_{B} is a scalar parameter that allows for gradual inelastic stiffness reduction of the element associated with plastification at end A and B. This term is equal to 1.0 when the element is elastic, and zero when a plastic hinge is formed. The parameter η is assumed to vary according to the parabolic function

$$\eta = 1.0 \quad \text{for } \alpha \leqslant 0.5 \tag{6a}$$

$$\eta = 4\alpha(1-\alpha) \quad \text{for } \alpha > 0.5 \tag{6b}$$

where α is a force-state parameter that measures the magnitude of axial force and bending moment at the element end. The term α in this study is expressed in a modified version of Orbison full plastification surface of cross-section, as presented by McGuire et al. (2000), as follows:

$$\alpha = p^2 + m_z^2 + m_y^4 + 3.5p^2m_z^2 + 3.0p^6m_y^2 + 4.5m_z^4m_y^2 \tag{7}$$

where $p = P/P_y$, $m_z = M_z/M_{pz}$ (strong-axis), $m_y = M_y/M_{py}$ (weak-axis). If the member forces violate yield condition, says $\alpha > 1$, the member forces will be corrected to return the yield surface along a path passing though the origin by the application of the bi-section method.

To treat the strain reversal effect in the hinge due to the abrupt change in applied direction of dynamic load, the scalar parameter η, which allows for gradual inelastic stiffness reduction of the element associated with plastification at member end as presented in Eq. (5), is modified based on the double modulus theory in Chen and Lui (1987) as follows:

$$\eta_{\mathrm{d}} = \sqrt{\eta_{\mathrm{d}y}\eta_{\mathrm{d}z}} \tag{8}$$

where

$$\eta_{\mathrm{d}y} = \frac{4\eta_0}{\left(1+\sqrt{\eta_0}\right)^2} \text{ for weak axis} \tag{9a}$$

$$\eta_{\mathrm{d}z} = \frac{2\eta_0}{1+\eta_0} \text{ for strong axis} \tag{9b}$$

2.4. Shear deformation effects

As presented by Kim et al. (2001), to account for transverse shear deformation effects in a beam-column element, the stiffness matrix may be modified as

$$\begin{Bmatrix} P \\ M_{y\mathrm{A}} \\ M_{y\mathrm{B}} \\ M_{z\mathrm{A}} \\ M_{z\mathrm{B}} \\ T \end{Bmatrix} = \begin{bmatrix} \frac{E_t A}{L} & 0 & 0 & 0 & 0 & 0 \\ 0 & C_{iiy} & C_{ijy} & 0 & 0 & 0 \\ 0 & C_{ijy} & C_{jjy} & 0 & 0 & 0 \\ 0 & 0 & 0 & C_{iiz} & C_{ijz} & 0 \\ 0 & 0 & 0 & C_{ijz} & C_{jjz} & 0 \\ 0 & 0 & 0 & 0 & 0 & \frac{GJ}{L} \end{bmatrix} \begin{Bmatrix} \delta \\ \theta_{y\mathrm{A}} \\ \theta_{y\mathrm{B}} \\ \theta_{z\mathrm{A}} \\ \theta_{z\mathrm{B}} \\ \phi \end{Bmatrix} \tag{10}$$

in which

$$C_{iiy} = \frac{k_{iiy}k_{jjy} - k_{ijy}^2 + k_{iiy}A_{\mathrm{s}z}GL}{k_{iiy} + k_{jjy} + 2k_{ijy} + A_{\mathrm{s}z}GL} \tag{11a}$$

$$C_{ijy} = \frac{-k_{iiy}k_{jjy} + k_{ijy}^2 + k_{ijy}A_{\mathrm{s}z}GL}{k_{iiy} + k_{jjy} + 2k_{ijy} + A_{\mathrm{s}z}GL} \tag{11b}$$

$$C_{jjy} = \frac{k_{iiy}k_{jjy} - k_{ijy}^2 + k_{jjy}A_{\mathrm{s}z}GL}{k_{iiy} + k_{jjy} + 2k_{ijy} + A_{\mathrm{s}z}GL} \tag{11c}$$

$$C_{iiz} = \frac{k_{iiz}k_{jjz} - k_{ijz}^2 + k_{iiz}A_{sy}GL}{k_{iiz} + k_{jjz} + 2k_{ijz} + A_{sy}GL} \tag{11d}$$

$$C_{ijz} = \frac{-k_{iiz}k_{jjz} + k_{ijz}^2 + k_{ijz}A_{sy}GL}{k_{iiz} + k_{jjz} + 2k_{ijz} + A_{sy}GL} \tag{11e}$$

$$C_{jjz} = \frac{k_{iiz}k_{jjz} - k_{ijz}^2 + k_{jjz}A_{sy}GL}{k_{iiz} + k_{jjz} + 2k_{ijz} + A_{sy}GL} \tag{11f}$$

where A_{sy} and A_{sz} are the shear areas with respect to y and z axes, respectively.

2.5. Vibration analysis

From Chopra (2001), in order to obtain the natural frequencies and vibration modes of three-dimensional steel frame, the following eigenproblem needs to be solved

$$[\mathbf{K}_0]\boldsymbol{\varphi} = \omega^2[\mathbf{M}]\boldsymbol{\varphi} \tag{12}$$

where $[\mathbf{K}_0]$ is the initial stiffness matrix, $[\mathbf{M}]$ is the common lumped mass matrix, $\boldsymbol{\varphi}$ is a mode shape, and ω is the circular frequency corresponding to $\boldsymbol{\varphi}$.

2.6. The equation of motion

The incremental form of the equation of motion for frames is given by

$$[\mathbf{M}][\Delta\ddot{\mathbf{u}}] + [\mathbf{C}][\Delta\dot{\mathbf{u}}] + [\mathbf{K}][\Delta\mathbf{u}] = [\Delta\mathbf{F}] \tag{13}$$

in which $[\mathbf{K}]$ is the stiffness matrix as mentioned earlier and $[\mathbf{C}] = a[\mathbf{M}] + b[\mathbf{K}_0]$ is the viscous damping matrix, where a and b are mass- and stiffness-proportional damping factors, respectively; $[\Delta\ddot{\mathbf{u}}]$, $[\Delta\dot{\mathbf{u}}]$, $[\Delta\mathbf{u}]$, and $[\Delta\mathbf{F}]$ are the incremental acceleration, velocity, displacement, and exciting force vectors, respectively, over a time increment of Δt. With the adoption of the Newmark method that was presented in Chopra (2001) for step-by-step solution of Eq. (13), the following equations are used

$$[{}^{t+\Delta t}\dot{\mathbf{u}}] = [{}^{t}\dot{\mathbf{u}}] + (1-\gamma)\Delta t[{}^{t}\ddot{\mathbf{u}}] + \gamma\Delta t[{}^{t+\Delta t}\ddot{\mathbf{u}}] \tag{14a}$$

$$[{}^{t+\Delta t}\mathbf{u}] = [{}^{t}\mathbf{u}] + \Delta t[{}^{t}\dot{\mathbf{u}}] + (0.5-\beta)(\Delta t)^2[{}^{t}\ddot{\mathbf{u}}] + \beta(\Delta t)^2[{}^{t+\Delta t}\ddot{\mathbf{u}}] \tag{14b}$$

in which $[{}^{t}\ddot{\mathbf{u}}]$, $[{}^{t}\dot{\mathbf{u}}]$, and $[{}^{t}\mathbf{u}]$ are the total acceleration, velocity, and displacement vectors at time t. The parameters β and γ define the variation of acceleration over a time step and determine the stability and accuracy characteristics of the method. Here β and γ are taken as 1/4 and 1/2 correspond to the assumption of the average acceleration method. Finally, the incremental equation of motion (13) can be expressed as

$$\left[[\mathbf{K}] + \frac{\gamma}{\beta\Delta t}[\mathbf{C}] + \frac{1}{\beta(\Delta t)^2}[\mathbf{M}]\right][{}^{t}\Delta\mathbf{u}] = [\Delta\mathbf{F}] + \left[\frac{1}{\beta\Delta t}[\mathbf{M}] + \frac{\gamma}{\beta}[\mathbf{C}]\right][{}^{t}\dot{\mathbf{u}}] + \left[\frac{1}{2\beta}[\mathbf{M}] + \Delta t\left(\frac{\gamma}{2\beta} - 1\right)[\mathbf{C}]\right][{}^{t}\ddot{\mathbf{u}}] \tag{15}$$

Once $[{}^{t}\Delta\mathbf{u}]$ is known, the remaining unknown vectors are computed as follows:

$$[{}^{t}\Delta\dot{\mathbf{u}}] = \frac{\gamma}{\beta\Delta t}[{}^{t}\Delta\mathbf{u}] - \frac{\gamma}{\beta}[{}^{t}\dot{\mathbf{u}}] + \Delta t\left(1 - \frac{\gamma}{2\beta}\right)[{}^{t}\ddot{\mathbf{u}}] \tag{16a}$$

$$[{}^{t}\Delta\ddot{\mathbf{u}}] = \frac{1}{\beta(\Delta t)^2}[{}^{t}\Delta\mathbf{u}] - \frac{1}{\beta\Delta t}[{}^{t}\dot{\mathbf{u}}] - \frac{1}{2\beta}[{}^{t}\ddot{\mathbf{u}}] \tag{16b}$$

$$[{}^{t+\Delta t}\mathbf{u}] = [{}^{t}\mathbf{u}] + [\Delta\mathbf{u}] \tag{16c}$$

$$[{}^{t+\Delta t}\dot{\mathbf{u}}] = [{}^{t}\dot{\mathbf{u}}] + [\Delta\dot{\mathbf{u}}] \tag{16d}$$

$$[{}^{t+\Delta t}\ddot{\mathbf{u}}] = [{}^{t}\ddot{\mathbf{u}}] + [\Delta\ddot{\mathbf{u}}] \tag{16e}$$

$$[{}^{t+\Delta t}\mathbf{F}] = [{}^{t}\mathbf{F}] + [\Delta\mathbf{F}] \tag{16f}$$

The procedure presented in equations (15) and (16) is repeated for the next time steps until the considered frame is collapsed or desired time duration ends.

3. Verifications

A computer program PAAP-Dyna is developed based on the above-mentioned formulation to predict vibration behavior of three-dimensional framed structures as well as its nonlinear response under earthquake loading. It is verified for validity using the results generated by ABAQUS program through three numerical examples. Although the use of shell element of ABAQUS can lead to extremely accurate results, it is not applied here because it is too time-consuming for such a nonlinear dynamic analysis. Therefore, the B33 beam element with 13 numerical integration points (five points in web, five in each flange) of ABAQUS is used to model framed structures herein. Four earthquake records of the El-Centro 1940, the Loma Prieta 1989, the Northridge 1994, and the San Fernando 1971, as presented in Fig. 1, are used as ground motion input data. Their peak ground accelerations and time steps are listed in Table 1. For each problem, the static load due to the weight of the mass and dead loading (if any) is applied first to the structure by a static analysis, and then the earthquake loading is applied by a dynamic time-history analysis. The mass- and stiffness-proportional damping factors are chosen based on first two modes of frame so that the equivalent viscous damping ratio is equal to 5%.

3.1. Two-storey three-dimensional frame for second-order effect verification

Fig. 2 shows the geometric and material properties of a two-storey three-dimensional frame with masses lumped at the framed nodes. The geometry of this frame is symmetric, but the mass distribution is not. The vertical concentrated loads applied at all framed nodes are chosen to be very large in order to show the second-order effect clearly. In numerical modeling, each framed element is divided into two equal elements.

After performing the vibration analysis, first two natural periods along the applied earthquake direction and corresponding mode shapes of the frame are obtained and compared in Table 2 and Fig. 3. It can be seen that a strong agreement of dynamic properties of the study frame generated by ABAQUS and proposed programs is obtained.

The roof displacement responses of frame and a comparison of their peak values and corresponding times of the linear elastic (LE) and second-order elastic (SE) analyses are shown in Fig. 4 and Table 3. As can be observed from those, the difference of displacement response of LE and SE analyses in each case

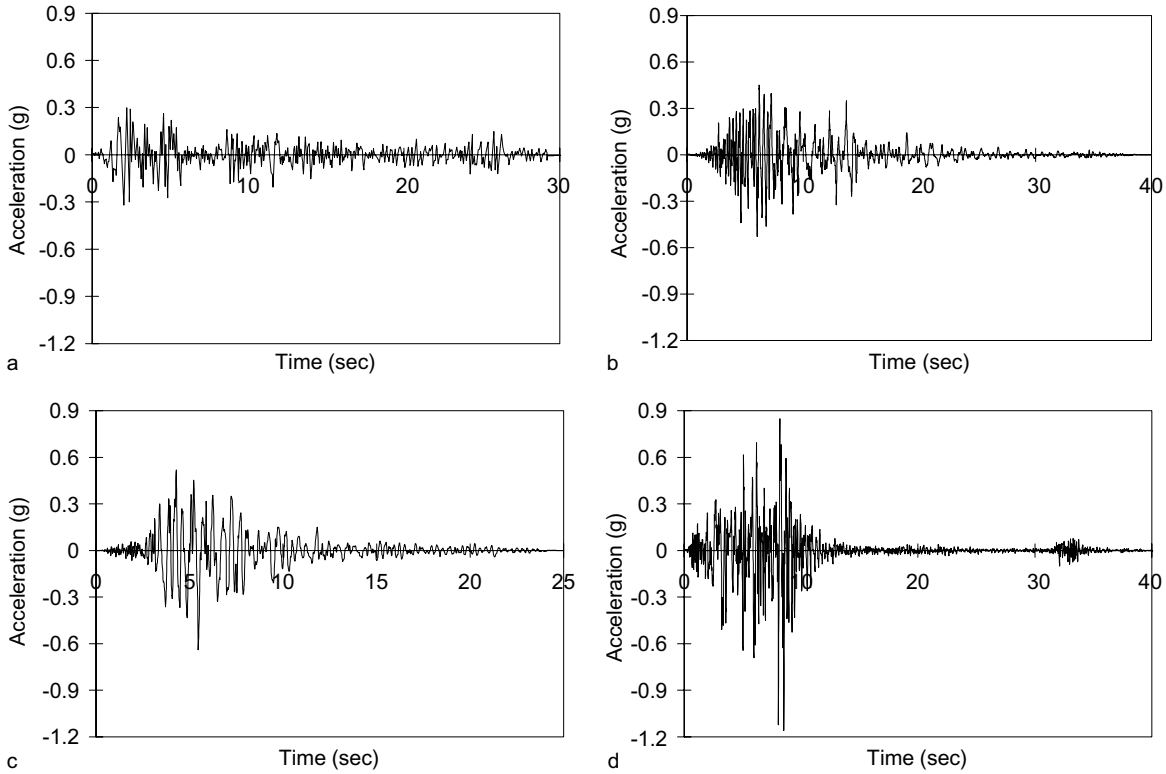

Fig. 1. Earthquake records: (a) El Centro (1940); (b) Loma Prieta (1989); (c) Northridge (1994) and (d) San Fernando (1971).

Table 1
Peak ground acceleration and its corresponding time step of the earthquake records

Earthquake	PGA (g)	Time step (s)
El Centro (1940) (Array, #9, USGS Station 117)	0.319	0.020
Loma Prieta (1989) (Capitola, 000, CDMG Station 47125)	0.529	0.005
Northridge (1994) (Simi Valley-Katherine, 090, USC Station 90055)	0.640	0.010
San Fernando (1971) (Pacoima Dam, 254, CDMG Station 279)	1.160	0.010

is distinct, and all results obtained by ABAQUS and the proposed programs are nearly the same, which prove the accuracy of the proposed program in predicting the second-order effect.

3.2. Verification examples of inelastic effect

3.2.1. Two-storey three-dimensional frame

The same structure, as presented in the previous example, is used here for verification, except for the application of vertical concentrated loads at framed nodes (Fig. 5). The roof displacement responses of the frame obtained from the second-order elastic (SE) and second-order inelastic (SI) analyses are shown in Fig. 6. A comparison of the peak roof displacement and its corresponding time is shown in Table 4. It is

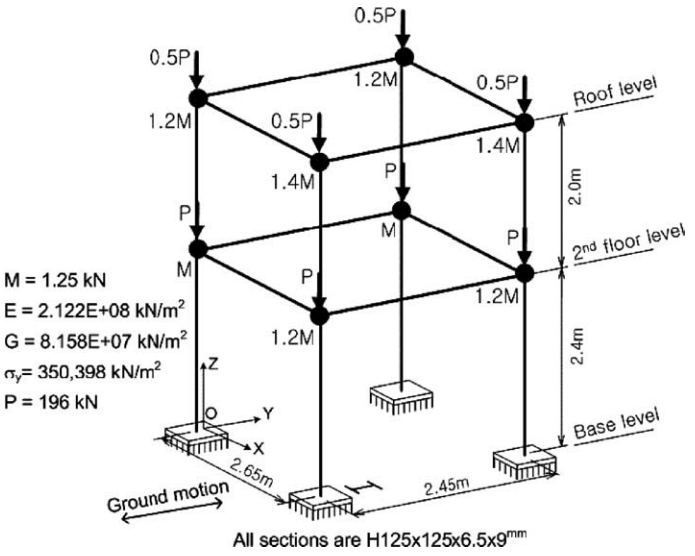

Fig. 2. Two-storey frame for second-order effect verification.

Table 2
Comparison of first two natural periods along the applied earthquake direction of two-storey frame

Mode	Period (s)		Error (%)
	ABAQUS	PAAP-Dyna (proposed)	
First	0.4340	0.4352	−0.28
Second	0.1217	0.1220	−0.32

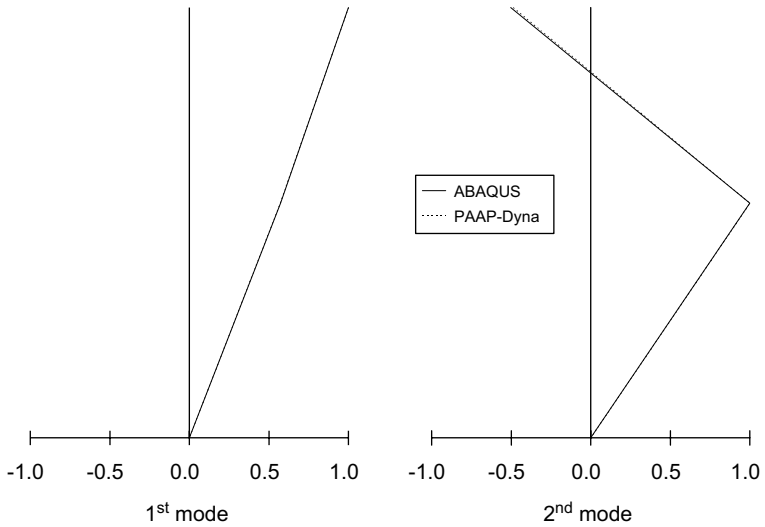

Fig. 3. Comparison of first two mode shapes along the applied earthquake direction of two-storey frame.

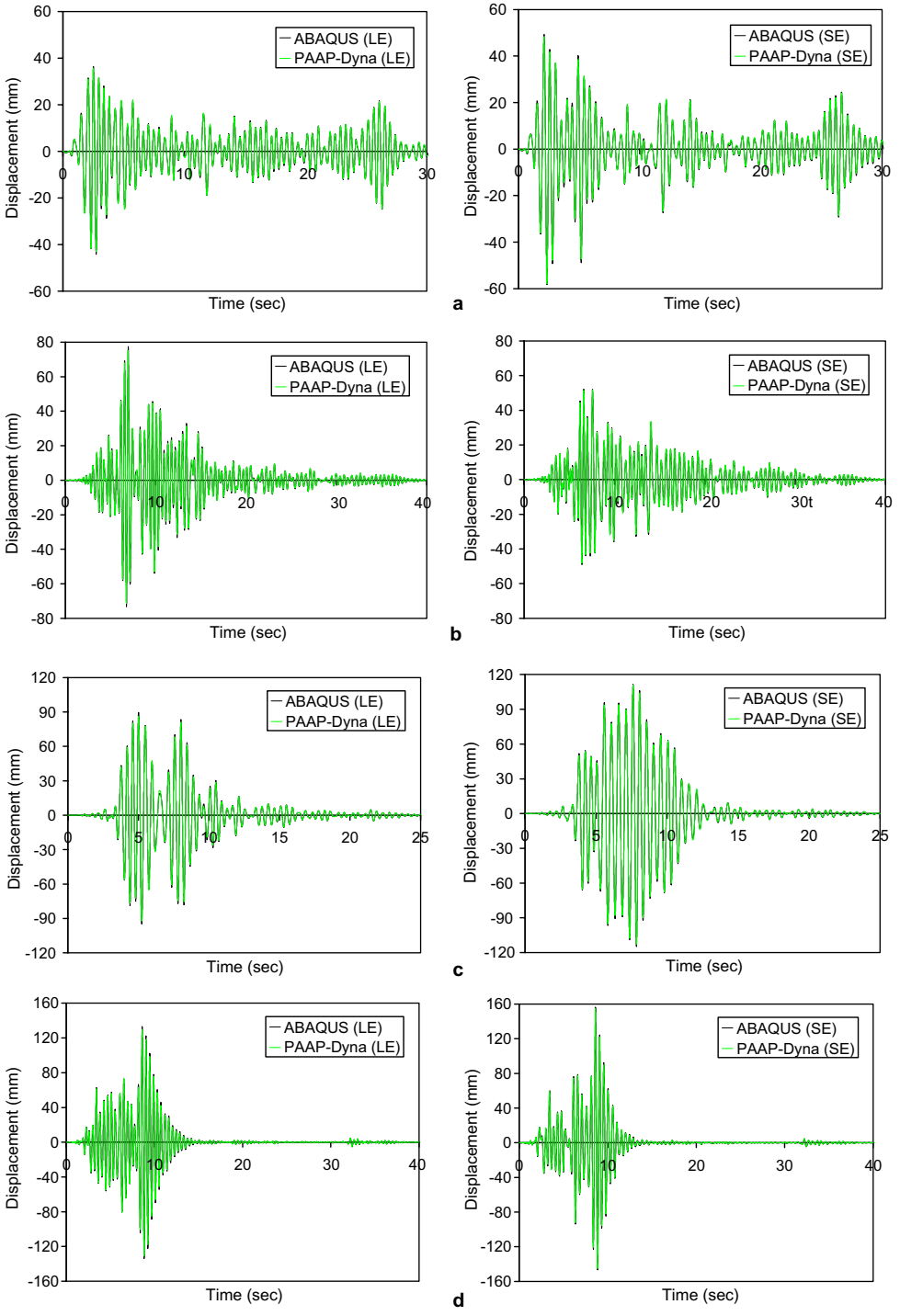

Fig. 4. Roof displacements of two-storey frame for second effect verification: (a) El Centro earthquake; (b) Loma Prieta earthquake; (c) Northridge earthquake and (d) San Fernando earthquake.

Table 3
Comparison of peak roof displacement and its corresponding time of two-storey frame for second-order effect verification

Eq. type	Min/max	Analysis type	ABAQUS		PAAP-Dyna (proposed)		Disp. Error (%)
			Disp. (mm)	Time (s)	Disp. (mm)	Time (s)	
El Centro	Max	LE	36.42	2.520	35.74	2.520	1.87
		SE	49.32	2.120	48.21	2.100	2.25
	Min	LE	−44.22	2.740	−42.98	2.740	2.80
		SE	−58.25	2.340	−57.86	2.340	0.67
Loma Prieta	Max	LE	77.41	6.950	75.07	6.940	3.02
		SE	52.14	7.565	51.90	7.555	0.46
	Min	LE	−73.13	6.755	−71.39	6.745	2.38
		SE	−49.10	6.385	−48.17	6.380	1.89
Northridge	Max	LE	89.63	5.010	86.38	5.010	3.63
		SE	111.45	7.600	110.71	7.600	0.66
	Min	LE	−94.73	5.230	−92.14	5.230	2.73
		SE	−114.57	7.840	−112.65	7.840	1.68
San Fernando	Max	LE	132.92	8.600	129.38	8.590	2.66
		SE	156.29	8.620	154.56	8.610	1.11
	Min	LE	−133.89	8.810	−130.89	8.800	2.24
		SE	−146.71	8.860	−145.24	8.840	1.00

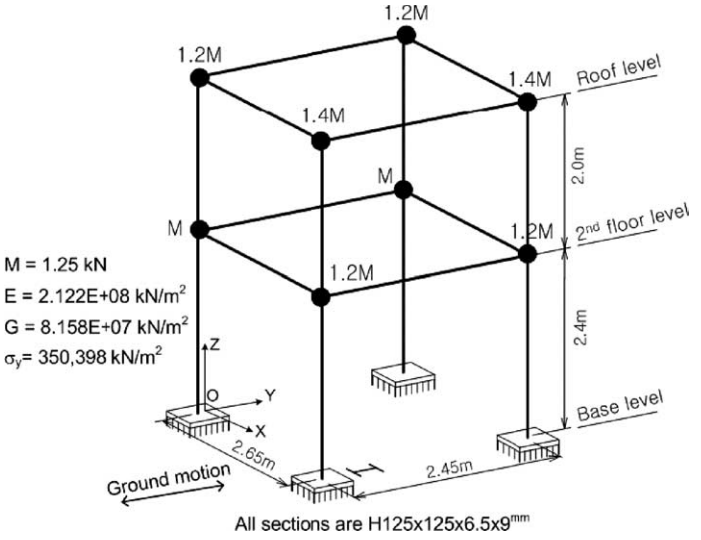

Fig. 5. Two-storey frame for inelastic effect verification.

observed that the ABAQUS and proposed programs give nearly identical results in all cases, including the slight permanent shifts in displacement due to inelastic behavior for SI analysis cases under Loma Prieta, Northridge, and San Fernando earthquakes. As is evident from the figure, the difference in displacement response of SE and SI analyses in these cases is relatively clear. For the case of El Centro earthquake having smallest PGA, it is noted that the displacement responses in SE and SI cases are almost identical, because the behavior of the framed structure is almost in elastic range in this case.

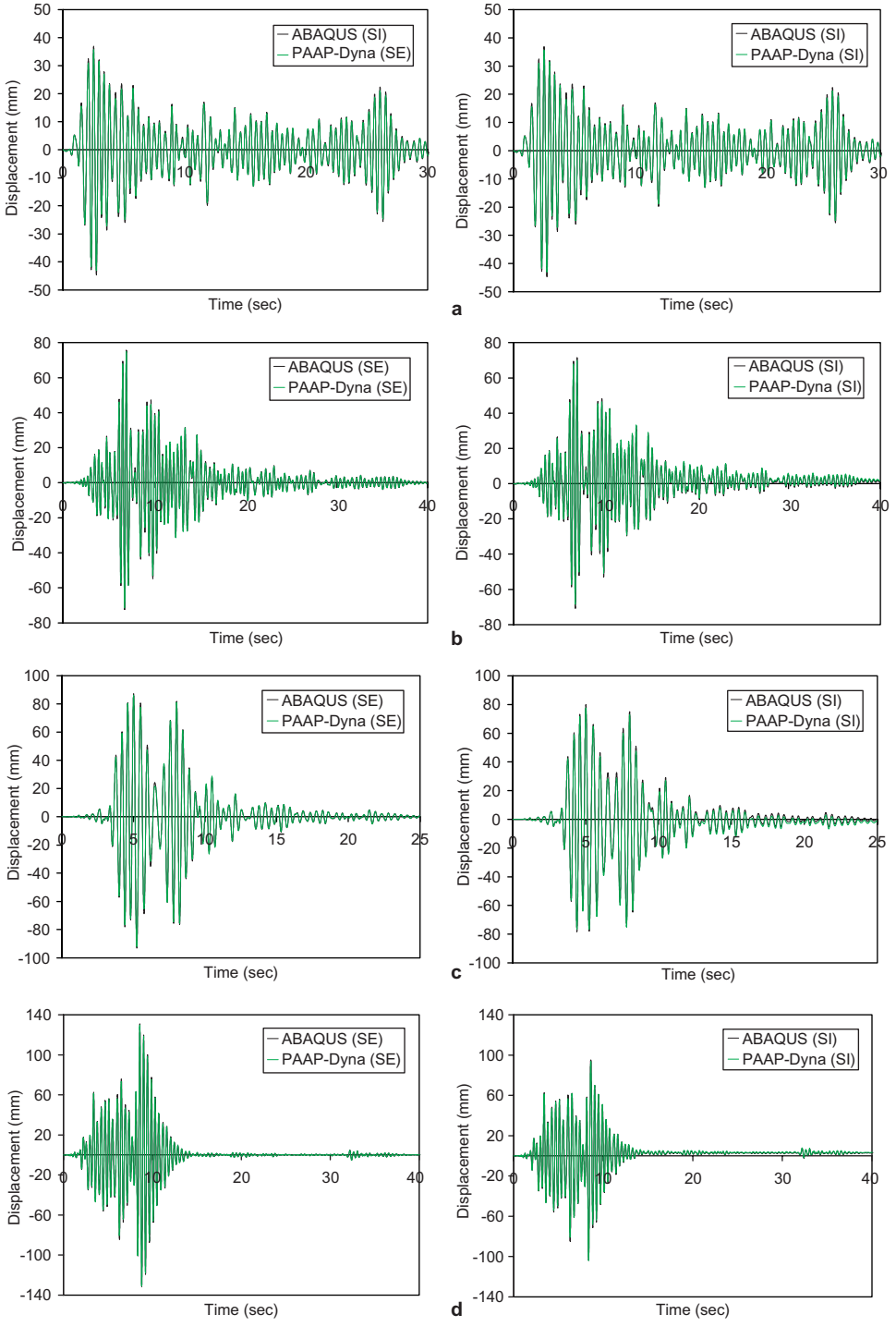

Fig. 6. Roof displacements of two-storey frame for inelastic effect verification: (a) El Centro earthquake; (b) Loma Prieta earthquake; (c) Northridge earthquake and (d) San Fernando earthquake.

Table 4
Comparison of peak roof displacement and its corresponding time of two-storey frame for inelastic effect verification

Eq. type	Min/max	Analysis type	ABAQUS		PAAP-Dyna (proposed)		Disp. Error (%)
			Disp. (mm)	Time (s)	Disp. (mm)	Time (s)	
El Centro	Max	SE	36.95	2.520	35.69	2.520	3.40
		SI	36.95	2.520	35.69	2.520	3.40
	Min	SE	−44.67	2.740	−43.02	2.740	3.68
		SI	−44.67	2.740	−43.02	2.740	3.68
Loma Prieta	Max	SE	75.62	6.950	74.97	6.940	0.86
		SI	71.49	6.950	69.87	6.940	2.28
	Min	SE	−72.46	6.755	−71.40	6.745	1.74
		SI	−70.71	6.755	−68.46	6.750	3.18
Northridge	Max	SE	87.38	5.010	86.24	5.010	1.28
		SI	79.98	5.010	77.77	5.010	2.77
	Min	SE	−93.07	5.240	−92.14	5.230	1.00
		SI	−78.22	4.400	−76.60	4.400	2.07
San Fernando	Max	SE	130.88	8.600	129.50	8.590	1.05
		SI	95.21	8.620	93.41	8.610	1.90
	Min	SE	−131.46	8.820	−131.08	8.800	0.29
		SI	−103.89	8.380	−103.84	8.370	0.04

3.2.2. *Four-storey three-dimensional frame*

This four-storey, two by two bay steel frame was presented by Campbell (1994). The framed geometry and members are kept to be same to the original frame, but the in-plane rigid slabs are neglected in modeling. Besides, because the original masses were too small, they are changed into bigger ones to be more realistic and to be capable of showing inelastic behavior clearly under earthquakes. The geometry, mass distribution, and material properties of the modified frame are shown in Fig. 7. Each member of the frame is only modeled by one element in numerical modeling.

A comparison of first three natural periods along the applied earthquake direction and their corresponding mode shapes of the four-storey frame obtained by vibration analysis of ABAQUS and the proposed programs are shown in Table 5 and Fig. 8. It can be seen that a very good correlation is found.

The roof displacement responses along X-axis of node A of the frame obtained by ABAQUS and proposed programs are shown in Fig. 9 for four different earthquakes. Their peak displacements and corresponding times are compared in Table 6. It is observed that except for the similar response in the cases of the frame subjected to the El Centro earthquake with the smallest PGA, the difference of displacement response of SE and SI analyses in the other cases is clear, and the obtained results correlate very well, including the permanent drifts of displacement in SI analysis cases. As in the previous example, this one also indicates that the proposed program is able to accurately predict displacements, which is an important index for a performance-based seismic design.

The locations of plastic hinges and their corresponding times at the most severe yielding state of this study frame subjected to Northridge and San Fernando earthquakes are shown in Fig. 10. It can be seen that the results obtained by ABAQUS and PAAP-Dyna are similar.

With using Intel Pentium IV 3.2 GHz, 2 GB RAM computer, the computational times of the ABAQUS and PAAP-Dyna programs for four-storey frame subjected to Loma-Prieta earthquake, which is the problem having the longest analysis time among four cases, are 12 h and 5 min, respectively. This result proves the high computational efficiency of the proposed computer program.

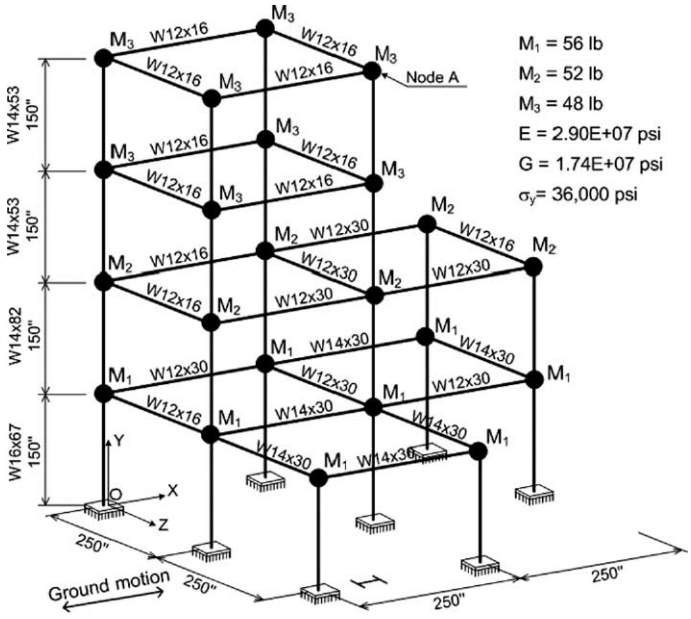

Fig. 7. Four-storey frame.

Table 5
Comparison of first three natural periods along the applied earthquake direction of four-storey frame (X direction)

Mode	Period (s)		Error (%)
	ABAQUS	PAAP-Dyna (proposed)	
First	1.1764	1.1746	0.15
Second	0.4077	0.4029	1.18
Third	0.1714	0.1707	0.41

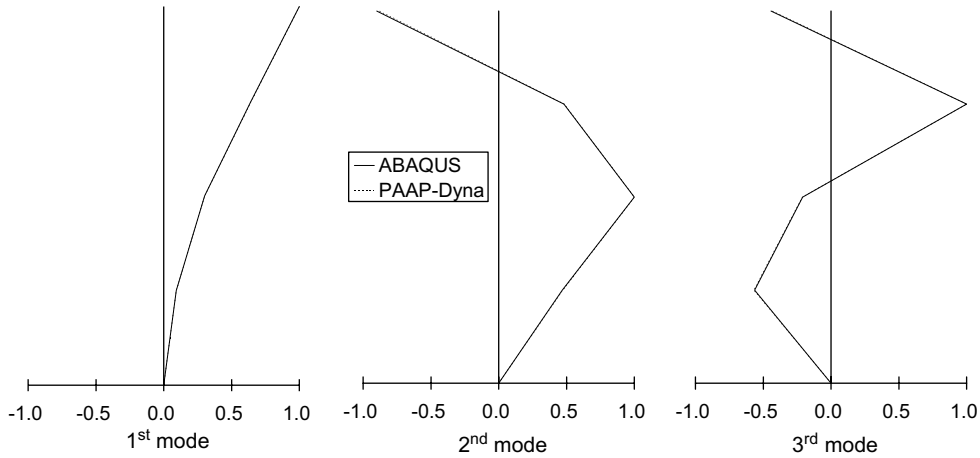

Fig. 8. Comparison of first three mode shapes along the applied earthquake direction of four-storey frame (X-direction).

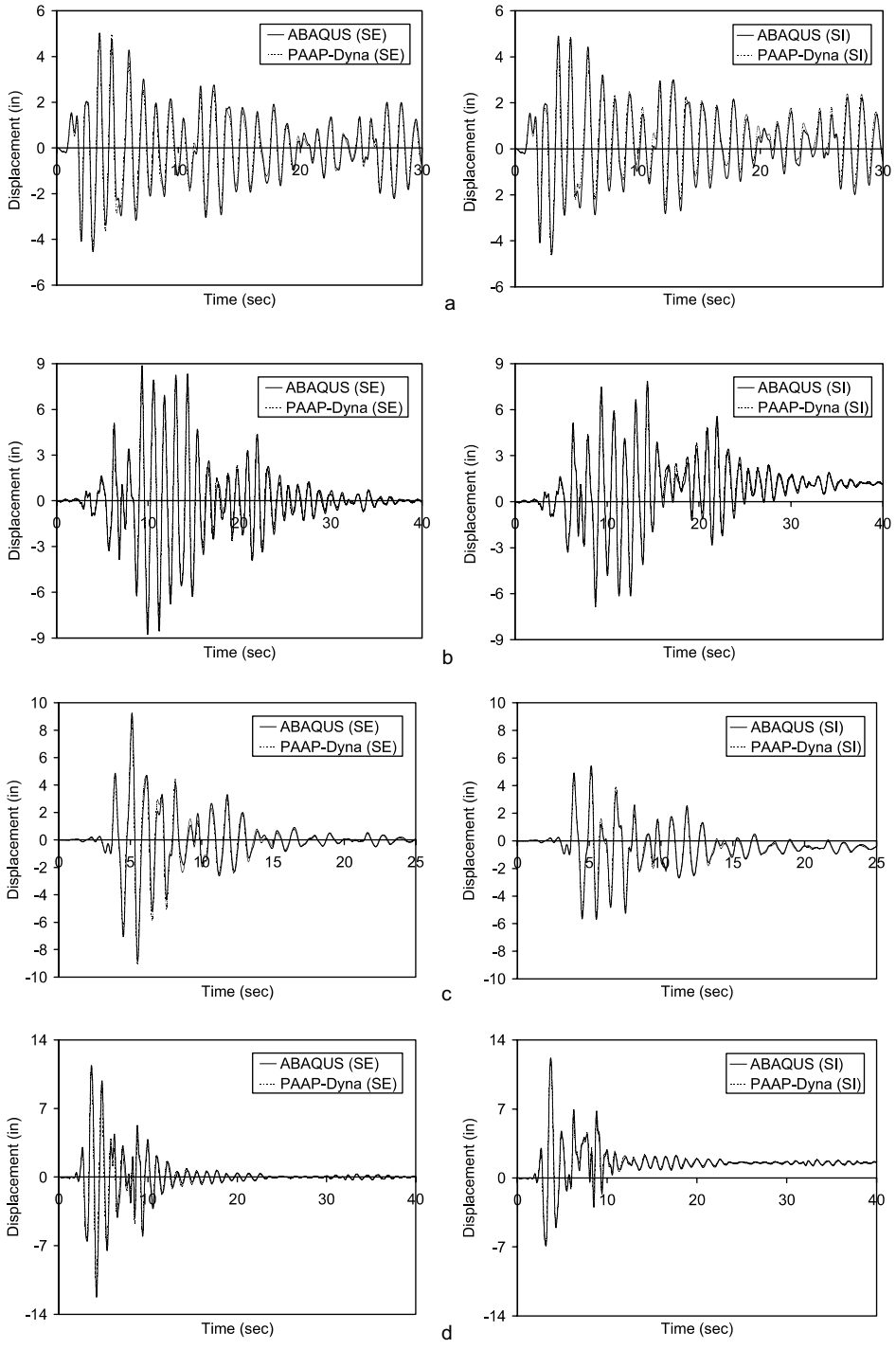

Fig. 9. Roof displacements at node A of four-storey frame: (a) El Centro earthquake; (b) Loma Prieta earthquake; (c) Northridge earthquake and (d) San Fernando earthquake.

Table 6
Comparison of peak roof displacement at node A and its corresponding time of four-storey frame

Eq. type	Min/max	Analysis type	ABAQUS		PAAP-Dyna (proposed)		Disp. error (%)
			Disp. (in)	Time (s)	Disp. (in)	Time (s)	
El Centro	Max	SE	5.013	3.520	5.042	3.500	−0.58
		SI	4.901	3.520	4.847	4.520	1.11
	Min	SE	−4.538	2.980	−4.458	2.960	1.75
		SI	−4.575	2.980	−4.612	2.960	−0.81
Loma Prieta	Max	SE	8.880	9.355	8.531	9.34	3.93
		SI	7.845	14.39	7.617	14.39	2.91
	Min	SE	−8.791	9.960	−8.535	9.960	2.91
		SI	−6.846	8.755	−6.490	8.750	5.21
Northridge	Max	SE	9.235	5.120	8.838	5.110	4.30
		SI	5.436	5.140	5.227	5.140	3.85
	Min	SE	−8.863	5.520	−9.064	5.510	−2.27
		SI	−5.694	5.500	−5.475	5.500	3.85
San Fernando	Max	SE	11.414	3.660	11.027	3.630	3.39
		SI	12.149	3.720	11.744	3.720	3.33
	Min	SE	−12.242	4.230	−12.045	4.200	1.61
		SI	−6.911	3.190	−6.804	3.170	1.54

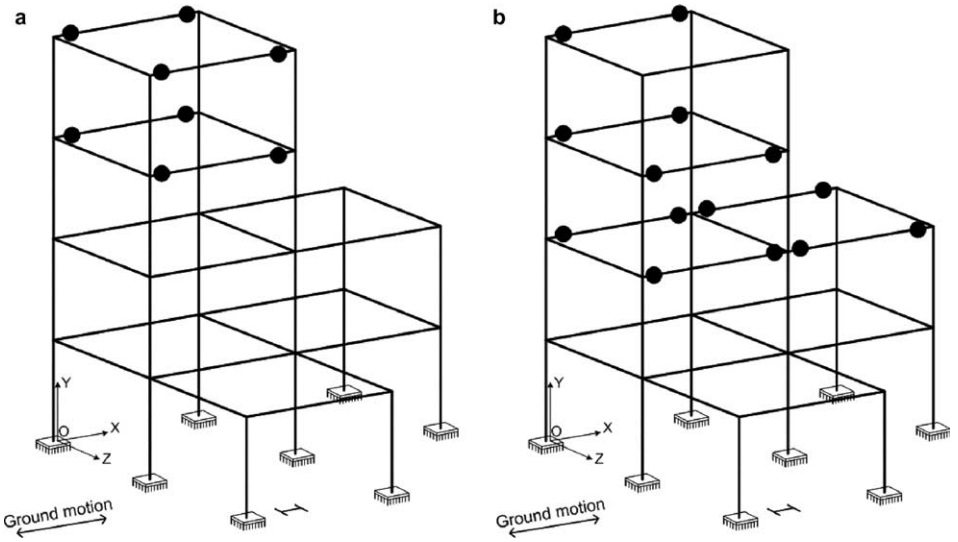

Fig. 10. Plastic hinge formation at the most severe yielding state of four-storey frame: (a) Northridge earthquake ABAQUS: $t = 5.50$ s; PAAP-Dyna, $t = 5.50$ s and (b) San Fernando earthquake: ABAQUS: $t = 3.72$ s; PAAP-Dyna, $t = 3.71$ s.

4. Conclusions

A simple and effective numerical procedure for the nonlinear dynamic time-history analysis of the three-dimensional steel frames considering both geometric and material nonlinearities has been presented. The computer program developed for this research is verified for accuracy and computational efficiency through

three numerical examples with four different earthquake loadings. It is also capable of accurately predicting natural periods and vibration mode shapes of framed structures. The good results obtained in a short analysis time prove that this computer program can effectively be used for office design in predicting nonlinear behavior of steel framed structures subjected to static and dynamic load instead of using the time-consuming and costly commercial structural software.

Acknowledgement

The work presented in this paper was supported by funds of National Research Laboratory Program (Grant No. M1-0204-00-0143-04-J00-00-083-10) from Ministry of Science and Technology in Korea. Authors wish to appreciate this financial support.

References

Al-Bermani, F.G.A., Zhu, K., 1996. Nonlinear elastoplastic analysis of spatial structures under dynamic loading using kinematic hardening models. Engineering Structures 18 (8), 568–576.

Campbell, S.D., 1994. Nonlinear elements for three dimensional frame analysis. Ph.D. Thesis, University of California at Berkeley, CA.

Chan, S.L., 1996. Large deflection dynamic analysis of space frames. Computer and Structures 58 (2), 381–387.

Chen, W.F., Lui, E.M., 1987. Structural Stability: Theory and Implementation. Elsevier, New York.

Chi, W.M., El-Tawil, S., Deierlein, G.G., Abel, J.F., 1998. Inelastic analyses of a 17-storey steel framed building damaged during Northridge. Engineering Structures 20 (4–6), 481–495.

Chopra, A.K., 2001. Dynamics of Structures: Theory and Applications to Earthquake Engineering. Prentice-Hall, New Jersey.

El-Tawil, S., Deierlein, G.G., 2001. Nonlinear analysis of mixed steel–concrete frames, Parts I and II. Journal of Structural Engineering 127 (6), 647–665.

Izzuddin, B.A., Smith, D.L., 1996. Large-displacement analysis of elastoplastic thin-walled frames, part I and II. Journal of Structural Engineering 122 (8), 905–925.

Jiang, X.M., Chen, H., Liew, J.Y.R., 2002. Spread-of-plasticity analysis of three-dimensional steel frames. Journal of Constructional Steel Research 58 (2), 193–212.

Kim, S.E., Lee, J., Park, J.S., 2002. 3-D second-order plastic-hinge analysis accounting for lateral torsional buckling. International Journal of Solids and Structures 39 (8), 2109–2128.

Kim, S.E., Lee, J., Park, J.S., 2003. 3-D second-order plastic-hinge analysis accounting for local buckling. Engineering Structures 25 (1), 81–90.

Kim, S.E., Park, M.H., Choi, S.H., 2001. Direct design of three-dimensional frames using practical advanced analysis. Engineering Structures 23 (11), 1491–1502.

Liew, J.Y.R., Chen, H., Shanmugam, N.E., Chen, W.F., 2000. Improved nonlinear plastic hinge analysis of space frame structures. Engineering Structures 22 (10), 1324–1338.

McGuire, W., Gallagher, R.H., Ziemian, R.D., 2000. Matrix Structural Analysis. John Wiley & Son, Inc., New York.

McKenna, F., Fenves, G.L., et al., 2005. Open system for earthquake engineering simulation (OpenSees). Available from: <http://opensees.berkeley.edu>. Pacific Earthquake Engineering Research Center, University of California, Berkeley.

Porter, F.L., Powell, G.H., 1971. Static and dynamic analysis of inelastic frame structures. Report No. EERC 71-3, University of California, Berkeley.

Teh, L.H., Clark, M.J., 1999. Plastic-zone analysis of 3D steel frames using beam elements. Journal of Structural Engineering 125 (11), 1328–1337.